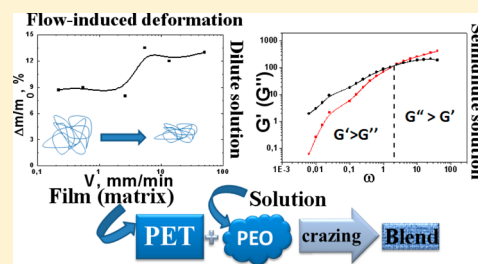


# Special Features of Crazing of Glassy Poly(ethylene terephthalate) in Poly(ethylene oxide) Solutions

Ekaterina G. Rukhlya,\*<sup>✉</sup> Evgeny A. Karpushkin, Larisa M. Yarysheva, and Alexander L. Volynskii

Faculty of Chemistry, M. V. Lomonosov Moscow State University, Moscow, Russia Federation 119991

**ABSTRACT:** The effect of the rate of PET deformation on the mechanism of penetration of flexible-chain macromolecules in the structure of crazes developing in PET has been considered. The penetration of the flexible-chain polymer in the porous structure is affected by the flow rate of the solute, the PEO solution characteristics (the concentration regime), and the porous structure parameters (porosity and pores radius of the crazed PET). PET films deformed via the crazing mechanism in solutions of PEO of different molecular mass have been examined. The influence of the concentration regime (dilute, semidilute unentangled, and semidilute entangled solutions) on the penetration of PEO in the forming porous PET structure has been demonstrated. In the case of PEO penetration from the dilute solution, a fraction of pores becomes accessible only under conditions of the flow-induced deformation at high rate of PET deformation. In the case of the semidilute entangled solution, at low deformation rate, PEO can penetrate in the forming porous PET structure via reptation motion. At the higher deformation rate, the fluctuation polymer network exhibits elastic behavior and cannot penetrate inside the porous PET structure via reptation.



## INTRODUCTION

Crazing is among basic types of plastic deformation of glassy and crystalline polymers. Orientation of polymer chains during crazing is a special phenomenon: macromolecules are oriented inside extremely thin (several nanometers in diameter) fibrillar aggregates separated by voids of comparable size. Such self-dispersing is especially efficient in the course of tension in adsorption-active liquid media. Many important features of crazing have been comprehensively studied and discussed in a number of reviews and treatises.<sup>1–6</sup>

A polymer generally exhibits significant (up to 60%) porosity upon the solvent crazing. This has been often utilized to incorporate various low-molecular-mass modifiers (dyes, repellents, bactericide agents, etc.) in polymers.<sup>6–8</sup>

In view of this, solvent crazing seems promising to prepare nanodisperse mixtures of incompatible polymers. However, it has been surmised that high viscosity of a polymer solution may prevent penetration of large macromolecular coils inside extremely small nanopores of crazed polymer. Therefore, nanodisperse mixtures of incompatible polymers have been conventionally prepared via *in situ* polymerization of a monomer inside a polymer matrix.<sup>9,10</sup>

At the same time, it has been demonstrated that a solution of poly(ethylene oxide) (PEO) with molecular mass as high as  $10^6$  can penetrate inside the nanoporous structure of crazes of poly(ethylene terephthalate) (PET).<sup>11,12</sup> Our research is focused on unique porous materials with the porous structure formed via the deformation in a polymer solution and investigation of simultaneous penetration of polymer solutions in the porous structure being developed. Understanding of the related processes is an important part of development of novel methods for the preparation of polymer blends during the tensile drawing of polymers in the solutions of other polymer

via the mechanism of crazing. The proposed approach is advantageous in that it does not require thermodynamic compatibility between components and can be used for quite different polymers and additives affording a wide range of polymer blends. In this report we will consider the effect of rate of PET deformation on the mechanism of PEO macromolecules penetration in the crazes being developed in the course of the process.

## EXPERIMENTAL SECTION

**Materials.** Amorphous nonoriented 100  $\mu\text{m}$  thick PET films were used as the matrix. PEO with molecular mass 4 kDa (PEO4K), 40 kDa (PEO40K), 400 kDa (PEO400K), and 1000 kDa (PEO1M) were used as the flexible-chain component. All the mentioned polymers with polydispersity index 1.1 were purchased from Aldrich. A water–ethanol mixture (1:7, v/v) was chosen as the adsorption-active medium, since ethanol is adsorption-active toward PET and facilitates the development of deformation via the crazing mechanism. Water is inert toward PET; however, its presence ensured the solubility of PEO.

**Sample Preparation: A PET–PEO Blend.** High-molecular-mass PEO is solid at room temperature; therefore, it can only be incorporated into a PET film being deformed via crazing from the solutions. In a typical experiment, a  $6.15 \times 20$  mm PET specimen immersed in a PEO solution was stretched at a constant strain rate (0.22–265.5 mm/min). A water–ethanol (1:7 v/v) mixture was used as solvent, and the PEO concentration was 5.5–30% (w/v) (5.5–30 g per 100 mL of the solution). The solvent-crazed samples (PEO–PET blends) were wiped off in order to remove residual PEO from the surface and then dried to constant mass under isometric conditions to completely remove the solvent.

Received: May 24, 2017

Revised: June 30, 2017

Published: July 7, 2017

**Calculation of Porosity.** The porosity  $W$  of the solvent-crazed PET was defined as relative volume change in the course of crazing:  $\frac{\Delta V}{V_0} = \frac{V_t - V_0}{V_0} \times 100\%$ , with  $V_t$  being the specimen volume after its tensile drawing and  $V_0$  being the starting specimen volume.

**Content of PEO in PET.** This was determined by weighing and defined as  $\frac{\Delta m}{m_0} = \frac{m_t - m_0}{m_0} \times 100\%$ , with  $m_0$  being the initial mass of a PET specimen and  $m_t$  standing for its mass after deformation in a PEO solution and drying.

**Pressure-Driven Liquid Permeability.** Porous structure of the solvent-crazed PET films was studied by means of pressure-driven liquid permeability toward the water–ethanol mixture using an FMO-2 membrane cell at a pressure of 2 MPa. The cell was modified so that the measurements in the presence of a liquid medium were possible, i.e., under the conditions preventing the specimen shrinkage after drawing. Thus, the so-determined effective pore diameter reflected the native structure of the crazed PET. The effective pores size ( $r$ ) in the crazes was calculated from the liquid permeability ( $G$ ) and the specimen volume porosity ( $W$ ) using the Pouseille equation:

$G = \frac{W r^2 S_0 \Delta P}{8 \eta d}$ , with  $\Delta P$ , the external pressure;  $d$ , the film thickness;  $\eta$ , the liquid viscosity; and  $S_0$ , the film area.

**Viscosity.** Relative viscosity of PEO solutions in a water–ethanol mixture was measured with an Ubbelohde viscometer (viscosity of the mixed solvent was 2.33 cps; no correction for kinetic energy was made). Prior to the measurements, the solutions were equilibrated at 20 °C for 15 min; the temperature was maintained constant within  $\pm 0.2$  °C.

**Light Scattering.** Light scattering of PEO solutions was measured with a Photocor Complex photometer (Photocor Instruments, USA) equipped with a He–Ne laser as the light source (10 mW,  $\lambda = 633$  nm, scattering angle 90°). PEO concentration in the solutions was 0.7 wt %. The solutions were filtered through Millipore porous filters with pore size 0.2  $\mu\text{m}$ . Hydrodynamic radius of the macromolecules  $R_h$  was calculated from the self-diffusion coefficient  $D$  data using the Einstein–Stokes equation,  $R_h = \frac{kT}{6\pi\eta D}$  with  $k$  being the Boltzmann's constant,  $T$  standing for absolute temperature, and other symbols having the same meaning as in the above equations.

**Correlation Length ( $\xi$ ).**  $\xi$  for PEO macromolecules in the aqueous–ethanolic solution was calculated using the equation for the flexible-chain polymers in a good solvent:  $\xi = R_h \left(\frac{c}{c^*}\right)^{-3/4}$ , with  $c^*$  being the crossover concentration (see below) and other symbols being explained above.

**Crossover Concentration.** We calculated the solutions intrinsic viscosity  $[\eta]$  by extrapolation of the reduced viscosity to infinite dilution. The crossover (or overlap) concentration  $c^*$  was calculated from the intrinsic viscosity data according to the Debye criterion  $c^* = [\eta]^{-1}$ .

**Entanglement Concentration ( $c^{**}$ ).** The concentration corresponding to the appearance of a network of entanglements involving all the macromolecules in a solution was determined from the inflection point in the plot of the solution reduced viscosity as a function of concentration.

**Viscoelastic Properties.** The viscoelastic properties of PEO solutions (storage  $G'$  and loss  $G''$  moduli) were measured by means of rotational rheometry in the forced oscillation stress control mode as functions of frequency using a RheoStress 600 rheometer (Haake). In a typical measurement, the frequency range was 0.1–100 Hz; the frequency window was extended by collecting the data at temperature 5–40 °C and building the master curve at the reference temperature (20 °C) taking advantage of time–temperature superposition. The plate–plate (35 mm) measuring cell was used, the gap was 200–500  $\mu\text{m}$  depending on the solution viscosity, and the stress was adjusted so that the amplitude fell in the linear viscoelasticity range as determined in the preliminary amplitude sweep test. In order to avoid the solvent evaporation during the measurement, the specimen was covered with thin layer of low-viscosity mineral oil. The oil viscosity was negligibly low as compared to that of the solutions; therefore, its contribution to

the measured torque was negligible. PEO with molecular mass 100, 400, and 1000 kDa was used; its concentrations was 5.5 or 18.6 wt %.

## RESULTS AND DISCUSSION

As far as mass transfer of macromolecules into nanoporous materials under confined conditions (when the macromolecule size is comparable or exceeds that of the pores) is concerned, the concentration regime of the solution penetrating in the pores is of primary importance.

Graessley has proposed classification of polymer solutions into different behavior regimes basing on the solute concentration and molar mass: dilute, semidilute unentangled, semidilute entangled, and concentrated entangled ones.<sup>13</sup> The overlap concentration  $c^*$  separates the dilute and semidilute unentangled regimes; the entanglement concentration  $c^{**}$  separates semidilute unentangled and semidilute entangled regimes. The existence of different regimes stems from enhancement of the intermolecular interactions with increasing polymer concentration. As a result, the concentration dependences of a polymer solution properties such as relaxation time, viscosity, and diffusion coefficient are significantly different depending on the concentration regime. Therefore, study of these polymer solution properties as functions of the concentration provides comprehensive insight into the polymer dynamics and the role of polymer interactions in different concentration regimes. The corresponding theories describing polymer dynamics are the Zimm model for the dilute regime, the Rouse model for the semidilute unentangled regime, and the Doi–Edwards tube model for the semidilute entangled and concentrated entangled regimes.<sup>14,15</sup>

In this work, we applied the crazing method to investigate the penetration of a flexible-chain polymer inside a porous matrix. Crazing of polymers in AAM is accompanied by appearance and development of numerous crazes with a high-disperse fibrillar-porous structure, the pores and fibrils size not exceeding 10 nm. It has been found that the rate of the adsorption-active liquid medium transport to the tip of the growing craze determines the rate of the crazes development and the very possibility of the polymer crazing. In turn, the rate of the liquid flow to the tip of the craze can be varied depending on the preset deformation rate.

Herein we will report and discuss the effect of the deformation rate and the flow mechanism on the penetration of PEO macromolecules inside the developing structure of crazed PET as studied in the following concentration regimes (Table 3; the studies of the PEO solutions have been reported by us earlier<sup>11,16</sup>).

**Dilute Solution ( $c \ll c^*$ ).** Let us consider the penetration of PEO inside the forming porous structure of PET from the dilute solution. The content of PEO in PET as a function of the PET deformation rate in 5.5 wt % solution of PEO4K is shown in Figure 1. As follows from the data in Table 1, the effective diameter of pores in the PET crazes (7.6–8.4 nm at 100% tensile strain) exceeded the hydrodynamic radius of PEO4K coil (1.3 nm)<sup>16</sup> and hence PEO4K should have freely penetrated inside the porous structure being formed. However, a sudden increase in the PEO content in the crazed PET was observed above certain tensile strain (Figure 1).

The marked behavior can be explained by the nonuniformity of the crazed polymer structure and, in particular, by the distribution of the pores size. In this case, the flexible-chain polymer solution could penetrate in larger pores at low deformation rate (i.e., at low shear flow rate). The increase in

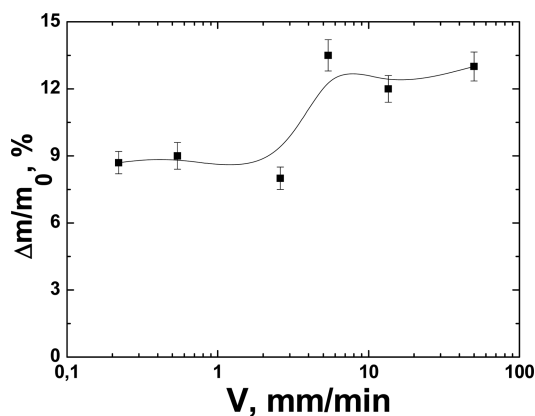


**Figure 1.** PEO content in solvent-crazed PET samples stretched by a tensile strain of 100% in a 5.5 wt % solution of PEO4K as a function of the deformation rate.

**Table 1. Effective Pore Diameter of the Crazes in PET Deformed in the Water–Ethanol Mixture**

$\epsilon$ , %	100	100	100
$d$ , nm	8.4	8.0	7.6
$v$ , mm/min	5.4	50	265.5

the deformation rate led to the increase in the flow rate of the polymer solution inside the forming crazes and enabled deformation, unfolding, and orientation of the coils in the solution.<sup>17</sup> As a result, smaller pores became accessible to the polymer solution, and the content of PEO in PET grew.

Indeed, macromolecules exist in the form of isolated coils in dilute solutions, and the polymer–polymer interactions are negligible. It is assumed that the mass transfer of macromolecules inside the nanopores from dilute solutions occurs via the translation mechanism, and the coil hydrodynamic radius  $R_h$  is a parameter of crucial importance. Polymer coils are considered hard spheres in the dilute solution, and their diffusion-driven (no external force) penetration in the pores is possible when the coil hydrodynamic radius does not exceed the pore size ( $r_p$ ),  $R_h \leq r_p$ .<sup>18</sup> The macromolecule penetration in the smaller pores is only possible under external force action, when the solvent flow exceeds certain critical value.<sup>17</sup> This threshold flow value is determined by a balance of friction between macromolecules and solvent and the elastic returning force of the polymer coil. If the flow rate is below the critical value, the friction force is not enough to drag the macromolecule inside the pore, and the latter is practically plugged. If the solvent flow rate is above the critical value, the flexible-chain polymer coils are deformed (the phenomenon known as flow-induced deformation), the chains are unfolded and oriented, and the macromolecule can penetrate inside the pore. The conditions for the flow-induced deformation in dilute solutions have been earlier considered: the flow-induced deformation does not occur when  $R_h/r_p = \vartheta < 0.5$ ,<sup>19,20</sup> and at  $\vartheta \geq 1$ , the macromolecules penetration in the pores is always accompanied by the flow-induced deformation.<sup>21–23</sup> Long and Anderson<sup>22</sup> postulated that when  $\vartheta > 1$ , apparently flow-induced deformation takes place, but when  $0.5 < \vartheta < 1$ , then the behavior of the polymer molecules is some sort of combination of deformation and rigid sphere sieving; the latter situation is very difficult to describe. In conclusion, if  $\vartheta > 0.6$ , flow-induced deformation plays an important role during the ultrafiltration of very dilute solutions of flexible polymers.<sup>24</sup>

Hence, our observations revealed that a fraction of the PET pores became available for PEO macromolecules penetration under conditions of flow-induced deformation, at high rate of PET deformation in PEO solution.

**Semidilute Entangled Solution ( $c > c^{**}$ ).** Let us consider the effect of the rate of PET deformation in semidilute entangled solutions of PEO of different molecular mass and concentration on the flexible-chain polymer penetration inside the developing fibrillar-porous structure of the crazes.

In contrast to the case of dilute PEO4K solution (Figure 1), no increase in PEO content in the porous PET matrix with the increase in the deformation rate was observed for the semidilute entangled PEO solutions; moreover, the PEO content in the crazed PET structure went down starting at certain deformation rate (Figure 2, curves 2–5).

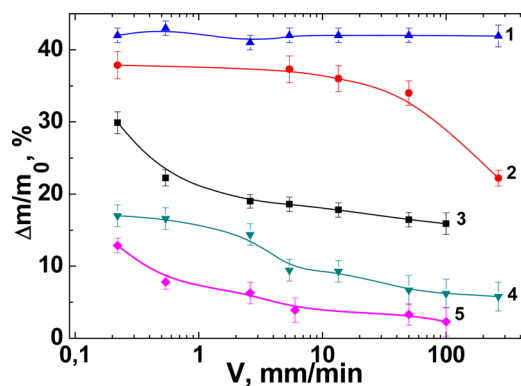


**Figure 2.** PEO content in solvent-crazed PET samples stretched by a tensile strain of 100% in a solution of PEO as a function of the deformation rate: 30 wt % PEO4K, curve 1; 20 wt % PEO40K, curve 2; 18.6 wt % PEO100K, curve 3; 9.3 wt % PEO100K, curve 4; 5.5 wt % PEO1M, curve 5.

Theory of macromolecules deformation in the flux is valid only for dilute polymer solutions, when the macromolecular coils do not interact with each other. With the increase in the polymer concentration up to the crossover threshold ( $c^*$ ), the chains motion is no longer independent, the coils are overlapped, and the fluctuation polymer network is formed (i.e., the solution behavior corresponds to the semidilute regime). Formation of the fluctuation polymer network starts around the crossover concentration  $c^*$  and continues up to the concentration of  $c^{**}$  corresponding to the transition of the polymer solution behavior to the regime of semidilute entangled solution with polymer entangled network. The  $c^{**}$  concentration marks the boundary between the translation and reptation flow mechanisms of the polymer solutions below and above this threshold, respectively. This brings the difference in the transport properties of macromolecules in the dilute and semidilute solutions.

The flow of semidilute solutions in the nanometer-range pores has been theoretically considered by Daoudi et al.<sup>25</sup> for the case of flexible-chain uncharged polymers, their dynamic behavior being well described by the scaling approach and the reptation model. For a semidilute polymer solution, a model of entangled network with the mesh size  $\xi$  corresponding to the blob size is considered. The mesh size is increased in the flow direction and reduced in the perpendicular direction. In this case, the blob size is the critical parameter rather than the size of the whole coil,  $\xi^\perp \leq d$ .<sup>14,15</sup> According to the data in Table 2,

**Table 2. Characteristics of PEO in the Water–Ethanol (1:7 v/v) Solution<sup>a</sup>**

PEO sample	$[\eta]$ , dL/g	$c^*$ , g/100 mL	$c^{**}$ , g/100 mL	$R_h$ , nm	$\xi$ , nm		
					$c = 5.5\%$	$c = 20\%$	$c = 30\%$
PEO4K	0.13	7.79	23.8	1.3		0.6	0.45
PEO40K	0.58	1.67	11.0	5.2	2.2	0.8	
PEO100K	1.0	1.00	7.1	9.2	2.5	1.0	
PEO400K	3.1	0.30	4.2	20	2.4	0.9	
PEO1M	6.6	0.20	1.4	>60			

<sup>a</sup>The data on intrinsic viscosity  $[\eta]$ , hydrodynamic coil radius  $R_h$ , crossover concentration  $c^*$ , entanglement concentration  $c^{**}$ , and the blob size  $\xi$  at different concentrations for the PEO used in this work are given in Table 2.

**Table 3. Concentration Regimes (in %) of PEO Solutions Investigated in This Study**

aqueous ethanolic solution	dilute ( $c < c^*$ )	semidilute unentangled ( $c^* < c < c^{**}$ )	semidilute entangled ( $c > c^{**}$ )
PEO4K	5.5	20	30
PEO40K		5.5	20
PEO100K		5.5	9.3, 18.6
PEO400K			5.5
PEO1M			5.5

the blob size for the studied PEO fractions was below the effective diameter of PET pores. In other words, PEO macromolecules of the studied molecular masses could freely penetrate via the reptation mechanism into the porous

structure being formed. However, the data in Figure 2 revealed that the PEO content depended on the rate of PET deformation in semidilute entangled PEO solutions; i.e., the penetration of PEO in the porous structure of PET was somewhat hindered.

The density of the fluctuation network (the number of entanglements per a macromolecule) formed by macromolecules in semidilute entangled polymer solutions depends on the solution concentration and the dissolved polymer molecular mass. This network is viscoelastic, and its behavior in tension is similar to that of a polymer gel,<sup>26–29</sup> i.e., a system containing permanent cross-links. In a viscoelastic system, the frequency (or the time scale) of shear force application is an important factor determining the rheological properties, in particular, the dominance of elastic or viscous behavior.

The de Gennes behavior of semidilute polymer solutions is observed at longer time scale (or lower frequency), where the loss modulus ( $G''$ ) is higher than the elastic one ( $G'$ ). In this case, the polymer chains have enough time to disentangle and slip by each other via reptation in response to the applied stress. A rubbery plateau region is found at higher frequency range where  $G'$  dominates over  $G''$ , being almost frequency-independent. Under these conditions, the polymer chains are deformed but not disentangled in response to the applied stress, thus giving rise to the returning force the cross-links, i.e., to the elastic behavior. The value of the angular frequency corresponding to the  $G'$  and  $G''$  intersection (marking the transition from the terminal zone behavior to the rubbery plateau) is equal to  $1/t_{\max}$ , with  $t_{\max}$  being the longest relaxation time or the time needed for around 63% of the stored elastic energy to be converted into viscous energy and dissipation. The

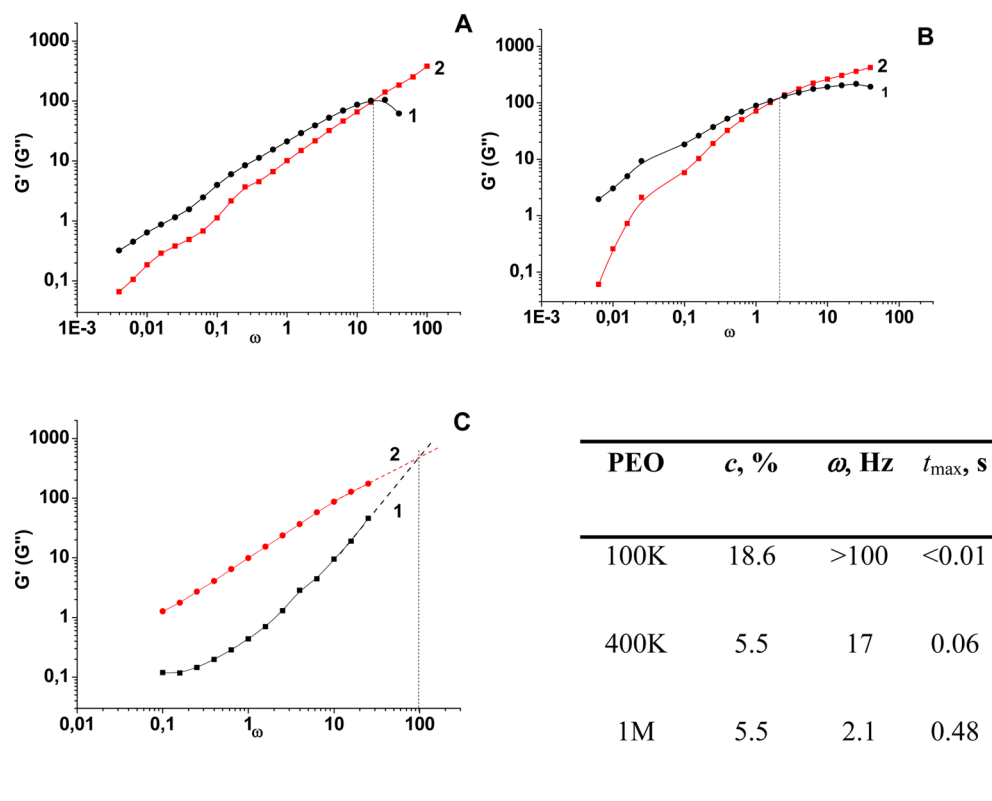


**Figure 3.** Elastic  $G'$  (1) and viscous  $G''$  (2) shear moduli of 5.5 wt % solutions of PEO400K (A), PEO1M (B), and 18.6 wt % solution of PEO100K (C). The table in the inset lists the inverse crossover frequencies and the corresponding longest relaxation times.



higher the molecular weight of the polymer or the higher its concentration in the solution, the longer the relaxation time. Therefore, the increase in the concentration of the solution or the molecular mass of the dissolved polymer shifts the intersection of the  $G'$  and  $G''$  curves toward lower frequency.

The viscoelastic behavior of the studied PEO solutions is shown in Figure 3. It is to be clearly seen that when the shear frequency was above a certain threshold, the elasticity modulus was higher than the viscous one, and the material was predominantly elastic. As expected, the moduli crossover was shifted to lower frequency (i.e., the transient network exhibited the elastic behavior over longer time scale) with the increase in PEO molecular mass and its concentration in the solution (cf. the inset table in Figure 3). The variation of the crossover frequency with PEO molecular mass and the solution concentration well exceeded an order of magnitude. Let us return to the data in Figure 2 and consider the penetration of PEO solutions in the forming porous structure of PET. It has been earlier shown<sup>6</sup> that the rate of the liquid (AAM, the PEO solution in this work) transport to the tip of the growing craze determines the rate of the craze development and the mere possibility of the polymer deformation via the crazing mechanism. In turn, the rate of the liquid flow to the craze tip is set by the polymer deformation rate. Altering the rate of the PET matrix deformation in the PEO solution led to the change of the liquid influx rate, i.e., the rate of the shear force acting on the PEO solution. As seen in Figure 2, the increase in the PEO molecular mass and its concentration in the solution led to the decrease in the PET deformation rate corresponding to the reduction of the PEO content in the porous PET matrix; those features were evidently in line with those observed in the direct rheological experiment (Figure 3).

In detail, solutions of PEO with the lowest molecular mass (PEO4K) penetrated inside the nanoporous structure being developed in PET over the whole range of the studied matrix deformation rate, and the PEO content was independent of the rate of the deformation. The increase in the PEO molecular mass to 40 kDa noticeably changed the dependence of the PEO content in the matrix as a function of the PET deformation rate (Figure 2, curve 2). At low deformation rate, entangled solution of PEO freely penetrated into the crazes. That was due to the fact that at low deformation rate (i.e., slow influx) the network cross-links behaved as transient ones and had no effect on the flexible-chain polymer penetration into the pores. However, at the deformation rate of 13.5 mm/min and higher, the content of PEO in the crazes of PET was noticeably reduced. Evidently, the entanglement network existing in the solution behaved as substantially elastic over that influx (i.e., shear) rate, hindering the PEO reptation into the nanosized pores. The drag effect of the macromolecular entanglement network was even more prominent for the solutions of PEO with higher molecular mass (PEO100K; Figure 2, curves 3 and 4). In the latter case, the horizontal part of the curve corresponding to the nearly stationary flow of PEO solution at low deformation rate nearly disappeared. The increase in the PEO100K concentration in the solution progressively hindered the macromolecules penetration into the nanoporous crazes structure over the whole probed range of the deformation rate; as a result, the PEO content in the developing crazes of PET was steadily decreasing with the increasing deformation rate.

Finally, in the case of PEO of the highest available molecular mass (PEO1M; Figure 2, curve 5), the entanglements network was so strong that the amount of PEO penetrating into the

crazes was decreasing over the whole range of the probed deformation rate.

In summary, at reasonably low rate of the matrix deformation, the flexible-chain polymer could penetrate in the forming porous structure of PET via the reptation mechanism. The increase in the deformation rate resulted in the increase in the influx rate, and the entangled polymer network became elastic, thus hindering PEO penetration inside the porous structure. As a result of the partially elastic response, the polymer solution could not penetrate through the whole cross section of the specimen, and the PEO content in the matrix was reduced. With the increase in the PEO molecular mass and its concentration in the solution, that elastic effect was manifested at lower rate of PET deformation (corresponding to slower influx of the PEO solution).

**Semidilute Unentangled Solution ( $c^* \ll c \ll c^{**}$ ).** Semidilute solutions of PEO with the concentration below the threshold of entangled network formation are complex systems, exhibiting the behavior similar to that of the dilute or semidilute solutions, depending on the PEO molecular mass and the solution concentration. Figure 4 shows the change of the PEO content in the PET deformed in the said AAM as functions of the deformation rate.

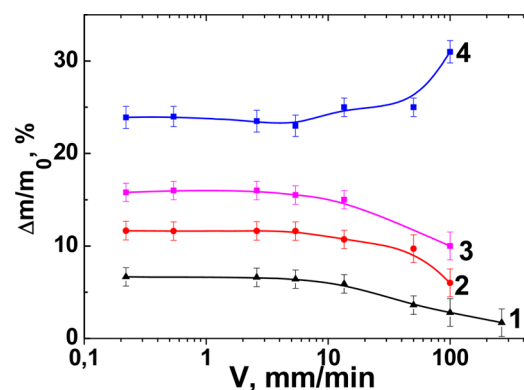


**Figure 4.** PEO content in solvent-crazed PET stretched by a tensile strain of 100% in a solution of PEO as a function of the deformation rate: 5.5 wt % PEO100K, curve 1; 5.5 wt % PEO40K, curve 2; 9.3 wt % PEO40K, curve 3; 20 wt % PEO4K, curve 4.

From the data presented in Figure 4 it is to be seen that solutions of PEO40K and PEO100K behaved similarly to the semidilute entangled solutions. In detail, the ranges of the deformation rate corresponding to the PEO content independent of the deformation rate and of the PEO content reduced with the increase in the deformation rate were observed. The origin of such behavior was analogous to that discussed above for the semidilute entangled solutions: the high deformation rate hindered the flexible-chain macromolecules reptation, and the transient network exhibited the elastic properties, thus preventing PEO penetration into the porous structure. The content of PEO4K in the PET matrix as a function of the deformation rate was different, revealing the increase above certain deformation rate. Such behavior was marked above as typical of the dilute PEO4K solution, the increase in the PEO content originating from the polydisperse distribution of the pores size in the formed porous structure. The increase in the deformation rate gave rise to the flow-induced deformation of PEO macromolecular coils, thus enabling the penetration of PEO into the smaller pores.

## CONCLUSION

In summary, we studied the features of PEO penetration in the forming porous PET structure as affected by the rate of the matrix deformation, concentration regime of the PEO solution, and molecular mass of PEO. The rate of the matrix deformation determined the flow rate of the polymer solution in the crazed PET structure. The fluctuating entanglements network in the PEO solutions, its properties being determined by the solute concentration and molecular mass, strongly affected the flexible-chain polymer transport inside the nanoporous structure of crazed PET. In the case of dilute solution, the entanglements network was not formed, and PEO penetration occurred via the translation mechanism; the PEO solution could penetrate in the larger pores at the low deformation rate, and the smaller pores became accessible at the increased deformation rate, in the flow-induced deformation regime. Under the latter conditions, PEO coils were deformed due to the external force action so that they could penetrate inside the smaller pores. The increase in either PEO concentration or molecular mass made its solution semidilute, and the penetration of PEO inside the pores was determined by the parameters of the fluctuating network. When PET was deformed at low rate in a semidilute entangled solution of PEO, the latter could penetrate inside the forming porous structure of PET via reptation, irrespectively of the pores size. When the deformation rate was increased, reptation of the fluctuating polymer network was no longer possible due to the elastic behavior which prevented PEO penetration inside the porous PET structure.

## AUTHOR INFORMATION

### Corresponding Author

\*E-mail [katrin310@yandex.ru](mailto:katrin310@yandex.ru) (E.G.R.).

### ORCID

Ekaterina G. Rukhlya: 0000-0001-5506-654X

### Notes

The authors declare no competing financial interest.

## ACKNOWLEDGMENTS

Research was financially supported by Russian Science Foundation (Grant # 17-13-01017).

## REFERENCES

- (1) Kambour, R. P. A Review of Crazing and Fracture in Thermoplastics. *Macromol. Rev.* **1973**, *7*, 1–173.
- (2) Michler, G. H. Crazing in Amorphous Polymers — Formation of Fibrillated Crazes Near the Glass Transition Temperature. In *Deformation and Fracture Behaviour of Polymers*; Grellmann, W., Seidler, S., Eds.; Springer: Berlin, 2001; pp 193–208.
- (3) Kramer, E. J. Crazing in Polymers. In *Microscopic and Molecular Fundamentals of Crazing*; Kausch, H. H., Ed.; Springer: Berlin, 1983; Vol. 52–53, pp 2–56.
- (4) Passaglia, E. Crazes and Fracture in Polymers. *J. Phys. Chem. Solids* **1987**, *48*, 1075–1100.
- (5) Earl, B. L.; Loneragan, R. J.; Johns, J. H. T.; Crook, M. Solvent Crazing of Polystyrene and Polymethylmethacrylate. *Polym. Eng. Sci.* **1973**, *13*, 390–394.
- (6) Volynskii, A. L.; Bakeev, N. F. *Surface Phenomena in the Structural and Mechanical Behaviour of Solid Polymers*; Taylor & Francis: London, 2016; p 536.
- (7) Bakeev, N. F.; Lukovkin, G. M.; Marcus, I.; Mikouchev, A. E.; Shitov, A. N.; Vanissum, E. B.; Volynskii, A. L. Imbibition Process WO1995009257A1, 1996.

- (8) Weichold, O.; Goel, P.; Lehmann, K.-H.; Möller, M. Solvent Crazed PET Fibers Imparting Antibacterial Activity by Release of Zn<sup>2+</sup>. *J. Appl. Polym. Sci.* **2009**, *112*, 2634–2640.

- (9) Sperling, L. H. *Interpenetrating Polymer Networks and Related Materials*; Springer US: Boston, MA, 1981.

- (10) Volynskii, A. L.; Bakeev, N. F. *Networks Based in Crystalline Polymers Deformed in Liquid Monomers*; Technomic Publishing: Lancaster, Basel, 1991; Vol. 3.

- (11) Rukhlya, E. G.; Litmanovich, E. A.; Dolinnyi, A. I.; Yarysheva, L. M.; Volynskii, A. L.; Bakeev, N. F. Penetration of Poly(ethylene oxide) into the Nanoporous Structure of the Solvent-Crazed Poly(ethylene terephthalate) Films. *Macromolecules* **2011**, *44*, 5262–5267.

- (12) Rukhlya, E. G.; Yarysheva, L. M.; Volynskii, A. L.; Bakeev, N. F. Incorporation of an Abnormally High Amount of Poly(Ethylene Glycol) into Poly(Ethylene Terephthalate) During Tensile Drawing in Liquid Media. *Polym. Sci., Ser. B* **2007**, *49*, 245–246.

- (13) Graessley, W. W. Polymer Chain Dimensions and the Dependence of Viscoelastic Properties on Concentration, Molecular Weight and Solvent Power. *Polymer* **1980**, *21*, 258–262.

- (14) de Gennes, P. G. *Scaling Concepts in Polymer Physics*; Cornell University Press: Ithaca, NY, 1979.

- (15) Doi, M.; Edwards, S. F. *The Theory of Polymer Dynamics*; Clarendon: Oxford, UK, 1986.

- (16) Rukhlya, E. G.; Yarysheva, L. M.; Volynskii, A. L.; Bakeev, N. F. Effects of Tensile Strain on the Peculiarities of PEO Penetration into the Nanoporous Structure of PET Deformed via the Crazing Mechanism. *Phys. Chem. Chem. Phys.* **2016**, *18*, 9396–9404.

- (17) Jin, F.; Wu, C. Observation of the First-Order Transition in Ultrafiltration of Flexible Linear Polymer Chains. *Phys. Rev. Lett.* **2006**, *96*, 237801.

- (18) Beerlage, M. A. M.; Peeters, J. M. M.; Nolten, J. A. M.; Mulder, M. H. V.; Strathmann, H. Hindered Diffusion of Flexible Polymers through Polyimide Ultrafiltration Membranes. *J. Appl. Polym. Sci.* **2000**, *75*, 1180–1193.

- (19) Mitchell, B. D.; Deen, W. M. Effect of Concentration on the Rejection Coefficients of Rigid Macromolecules in Track-Etch Membranes. *J. Colloid Interface Sci.* **1986**, *113*, 132–142.

- (20) Liu, T.; Xu, S.; Zhang, D.; Sourirajan, S.; Matsuura, T. Pore size and pore size distribution on the surface of polyethersulfone hollow fiber membranes. *Desalination* **1991**, *85*, 1–12.

- (21) Nguyen, Q. T.; Neel, J. Characterization of Ultrafiltration Membranes. 4. Influence of the Deformation of Macromolecular Solutes on the Transport Through Ultrafiltration Membranes. *J. Membr. Sci.* **1983**, *14*, 111–128.

- (22) Long, T. D.; Anderson, J. L. Effects of Solvent Goodness and Polymer Concentration on Rejection of Polystyrene From Small Pores. *J. Polym. Sci., Polym. Phys. Ed.* **1985**, *23*, 191–197.

- (23) Zeman, L.; Wales, M. Steric rejection of polymeric solutes by membranes with uniform pore size distributions. *Sep. Sci. Technol.* **1981**, *16*, 275–290.

- (24) Beerlage, M. A. M.; Heijnen, M. L.; Mulder, M. H. V.; Smolders, C. A.; Strathmann, H. Non-Aqueous Retention Measurements: Ultrafiltration Behaviour of Polystyrene Solutions and Colloidal Silver Particles. *J. Membr. Sci.* **1996**, *113*, 259–273.

- (25) Daoudi, S.; Brochard, F. Flows of Flexible Polymer Solutions in Pores. *Macromolecules* **1978**, *11*, 751.

- (26) Pearson, D.; Herbolzheimer, E.; Grizzuti, N.; Marrucci, G. Transient Behavior of Entangled Polymers at High Shear Rates. *J. Polym. Sci., Part B: Polym. Phys.* **1991**, *29*, 1589–1597.

- (27) Graham, R. S.; Likhtman, A. E.; McLeish, T. C. B.; Milner, S. T. Microscopic Theory of Linear, Entangled Polymer Chains Under Rapid Deformation Including Chain Stretch and Convective Constraint Release. *J. Rheol.* **2003**, *47*, 1171–1200.

- (28) Osaki, K.; Inoue, T.; Uematsu, T. Stress Overshoot of Polymer Solutions at High Rates of Shear: Semidilute Polystyrene Solutions with and without Chain Entanglement. *J. Polym. Sci., Part B: Polym. Phys.* **2000**, *38*, 3271–3276.

- (29) Chow, A.; Keller, A.; Mueller, A. J.; Odell, J. A. Entanglements in Polymer Solutions Under Elongational Flow: A Combined Study of

Chain Stretching, Flow Velocimetry and Elongational Viscosity.  
*Macromolecules* **1988**, *21*, 250–256.